

## Synchronized oscillations in swarms of nematode *Turbatrix aceti* Supplemental material

Anton Peshkov, Sonia McGaffigan, and Alice C. Quillen  
*Department of Physics and Astronomy, University of Rochester, Rochester, NY 14627, USA*

### I. NOTATIONS

Following the customary convention, we use throughout the article and the supplemental material the  $mean \pm se$  notation to indicate the standard mean error and the  $mean(sd)$  notation to indicate the standard deviation.

### II. EXPERIMENTAL METHODS

We obtained the starter cultures of *T. aceti* from two different aquarium supplies stores, to verify that the observed behavior wasn't particular to a specific strain. We grow these populations in a 1:1 solution of water and food grade apple cider vinegar at  $\sim 5\%$  acidity in which we put slices of apples as a food source. The population of nematodes in the culture reaches a peak density after one to two months, and stays relatively constant afterward. We have observed that *T. aceti* can successfully survive for many days with limited access to food and oxygen. The reproduction cycle of *T. aceti* takes many days and they can have a lifespan of up to two months [1]. Neither the motility nor the number of nematodes significantly varies for the duration of our experiments of a few hours.

We do not perform any generation control, which mean that nematodes at different stages of development, and therefore size, are present in the studied solutions.

For each experiment, 7-14 ml of nematode culture at peak density, is centrifuged for 3-5 minutes at an acceleration of 1700-4700 g. The concentrated blob of nematodes at the bottom of the tube is extracted and mechanically separated with a pipette to obtain a homogeneous high-density solution of nematodes. The studied densities  $d$  in the initial droplet ranged from 10 to 100 nematodes per  $\mu\text{l}$ . We study these high density droplets by depositing them on a glass slide with volumes in the range of 50-1000  $\mu\text{l}$ . Below the smallest 50  $\mu\text{l}$  volume, the droplet radius is similar to the length of a single nematode. Therefore the number  $N$  of nematodes in each droplet is in the range of 1-100 thousand organisms. For experiments in distilled water, the blob of nematodes from the first centrifugation was transferred to a tube with filled with 14 ml of distilled water and centrifuged again. Therefore we estimate the concentration of vinegar in this solution to be of the order of 0.1 – 0.2%.

For all the experiments we have coated the glass slide with a hydrophobic solution of Rain-X which contains polydimethylsiloxane (PDMS) as the main active ingredient. First, this allows the drops to have an initial contact angle around  $90^\circ$ . This enables study of the whole range of possible contact angles during evaporation. Secondly, the shape of the droplet on a hydrophobic surface is very close to circular, facilitating measurement of the drop diameter and contact angle. In contrast, the contact line can be irregularly shaped on wettable surfaces.

The experiments were performed in a room with a controlled temperature of 21(1)  $^\circ\text{C}$  and humidity 15(5)%. However, the temperature in the vicinity of the droplet, and therefore evaporation rate, is mostly dependent on the used illumination. For the Figure 1 of the main article, the droplet was illuminated from the bottom for better contrast and homogeneity of the image. However, for experiments where the determination of the droplet contact angle was important, the droplet was illuminated from top/side, to clearly delimit the border. While it is known that nematodes such as *C. elegans* are sensitive to light [2], we did not observe any dependence of the results presented in this article to the intensity or placement of the light source except for cases of extremely bright and close light sources. In the latter case, we observed the concentration of nematodes on the side opposite to the light source. However we believe that the nematodes avoided heat rather than light.

### III. DATA ANALYSIS

#### A. Characterization of the metachronal wave

To characterize the metachronal wave we recorded the droplets from the top with frame rates going from 30 to 60 fps. Parameters, such as the oscillation frequency, the metachronal wave speed, and the velocity of displacement of nematodes were obtained by visual extraction from several dozens to few hundreds consecutive frames (corresponding to a few minutes of recording).

To determine the time of the percolation of the metachronal wave, we visually analyzed the recording to determine the time at which the nematodes started to oscillate synchronously on the whole perimeter of the droplet. The error on the determination time of the metachronal wave percolation can be estimated of at most a couple of minutes. This time interval would correspond to an error on the contact angle of the droplet of less than  $1^\circ$ , smaller than the error on the determination of the angle itself as explained in the next section.

## B. Drop shape determination

The relatively large size of our droplets implies that the gravity force deforms the droplet surface. A spherical approximation for the drop shape for the contact angle determination is not accurate. Instead we adopt an ellipse approximation to measure the contact angle for the smaller ( $\leq 100\mu\text{l}$ ) droplets, using the ImageJ “Contact angle” plugin, and B-splines fitting [3] for droplets of all sizes, using the ImageJ “DropSnake” plugin. In theory, the axisymmetric drop shape analysis (ADSA) method[4] should give the best results for our droplets as it fits an analytical equation to the data. In practice the built-in artificial limitations on acceptable parameters in the ImageJ “LB-ADSA” plugin[5] were preventing us to obtain a correct fitting in a lot of cases. We were sometime successful in obtaining good results with the DropUI program[6] which is also based on the ADSA method. However, the impossibility of manually defining the droplet surface, and the regular failure of the automatic algorithm to detect it correctly, precluded us from using this program for analysis of the majority of our droplets.

Figure 1 presents a comparison of the extracted contact angles for the  $150\mu\text{l}$  droplet from Figure 2. b) in the main text, using the three approaches described above. We can see that the elliptical approximation slightly overestimate the contact angle as compared to the two other approaches. This can be explained by the relatively large drop size, where the elliptical approximation is less accurate. Nevertheless, the angle obtained by the different methods are in reasonable agreement. While spline fitting give the “noisiest” results, it’s the method that worked for all of our droplets and therefore the one we used most frequently. We note that measuring angles below  $\sim 20^\circ$ , is very error-prone, being highly dependent on the alignment of the camera. However, such small angles are mostly outside of our interest in this article.

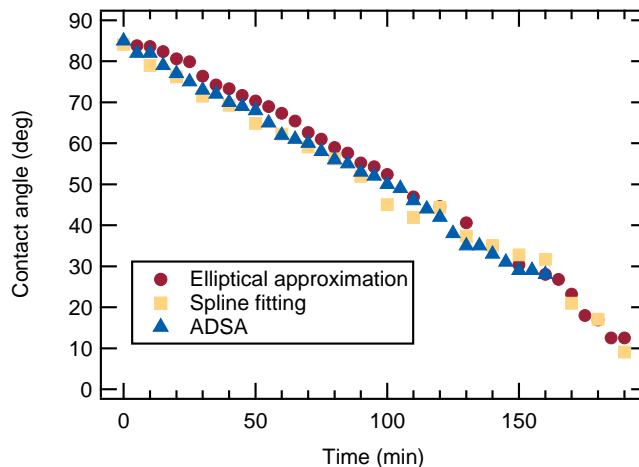


Figure 1. Contact angle of a  $150\mu\text{l}$  initial volume evaporating droplet as a function of time as extracted with three different measurement methods. Red circles, elliptical approximation using the ImageJ “Contact angle” plugin. Yellow squares, B-spline fitting using the ImageJ “DropSnake” plugin. Blue triangles, ADSA method using the DropUI program.

From Figure 1 we estimate a standard deviation of  $4.2^\circ$  and a standard mean error of  $1.2^\circ$  for the extracted contact angles in the main article taking into account the most error-prone elliptical approximation. This uncertainty does not affect our results or conclusions. Note that the the angle extraction for the third part of the article was done using exclusively the ImageJ “LB-ADSA” plugin, for which we estimate a much smaller standard deviation of  $1^\circ$ . The diameter of the droplets were obtained from the droplet surface approximation by the B-spline fitting of the DropSnake plugin or the ADSA fitting of LB-ADSA plugin. We estimate a small standard deviation of  $0.1\text{ mm}$  for the diameter.

### C. Nematode Density determination

To determine the initial density of nematodes, we diluted the dense nematode suspension 10-50 times in a 50:1 solution of water and glycerol to prevent droplet diameter shrinkage during evaporation. 10  $\mu\text{l}$  droplets of the diluted solution were placed on a glass slide and evaporated. The number of nematodes in each droplet was then manually counted under a microscope. This provides the mean and the error estimate for the initial density.

The number of nematodes per unit length oscillating near the border in Figure 2. b) was obtained by manually counting the number of oscillating nematodes near the border in 5-7 frames separated by 5 second intervals in the vicinity of each contact angle providing the mean and error estimate.

## IV. INSTABILITIES AND MULTIPLE WAVES

### A. Wave stability

In the smaller droplets ( $< 500 \mu\text{l}$ ), the metachronal wave, once formed, appears to be stable until its disappearance, when the drop completely evaporates. In rare cases we observed a temporal dramatic increase in the size of the central cluster, which leads to the depletion of the nematodes on the border and a temporal disappearance of the metachronal wave.

In larger droplets ( $> 500 \mu\text{l}$ ), we observed that the metachronal wave can sometimes split into several parts with opposite rotating directions (see supplemental video SM7) and even fully reverse the direction of rotation along the whole border. Two possible explanations can be given to that phenomenon. First, that above some instability length of the border  $L_i \approx 50\text{mm}$ , the wave becomes unstable due to an instability in the process of synchronization. Another explanation may be due to external properties of the droplet. The droplet slightly shrinks during evaporation, and given the non-perfect nature of the substrate, this shrinkage is not equivalent in all radial directions. This would lead to the deformation of the border and a potential nucleation of a “defect” in the wave. For larger droplets, the probability of a substantial deformation of the border is naturally higher.

### B. Multiple waves

Note that since the amplitude of oscillation for an individual nematode is approximately 0.1 mm, the nematodes cannot oscillate in the plane perpendicular to the bottom surface of the drop. Therefore, the oscillations will be increasingly confined to the bottom surface plane as the contact angle decreases. This is indeed what we experimentally observe. If the contact angle of the droplet becomes really small, one may wonder if the confinement can induce the metachronal wave more distant from the droplet border. Indeed, for very small contact angles, we sometimes observed the creation of a secondary wave in the inner radius as can be seen in the supplemental movie SM8. This wave is always counter-rotating as compared to the border wave. This is easy to understand, if the nematodes rotated in the same direction, they will just penetrate inside the border wave, the only way for such wave to exist is to rotate in the opposite direction. However, such double waves are relatively short living, inevitably leading to the perturbation of the outer wave, and even sometimes to the reversal of the direction of the latter.

## V. ESTIMATION OF THE FORCE EXERTED BY THE NEMATODE ON THE DROP SURFACE

We have seen that the force produced by the nematodes is sufficient to deform the surface of the droplet. We can estimate the force on the surface based on the pressure required for surface deformation with the wavelength of the metachronal wave. The metachronal wave has a typical wavelength  $\lambda_w \sim 1 \text{ mm}$  and amplitude  $A_w \sim 0.1 \text{ mm}$  (Figure 2). We describe the surface with a height away from the mean  $\xi = A_w \cos k_w x$  where  $x$  is a distance along the surface and wave vector  $k_w = 2\pi/\lambda_w$ . The pressure difference can be estimated from the curvature of the surface

$$\begin{aligned} \Delta p &\sim \gamma_l g \frac{d^2 \xi}{dx^2} = \gamma_l g A_w k_w^2 & (1) \\ &\sim 287 \mu\text{N}/\text{mm}^{-2} & (2) \end{aligned}$$

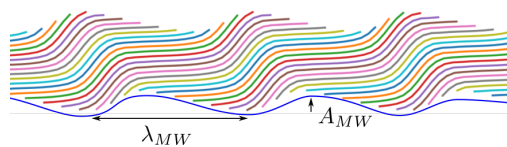


Figure 2. Diagram of the wave wavelength  $\lambda_W$  and amplitude  $A_w$ .

To estimate force per nematode we need to estimate the number of them per unit area near the surface. If we adopt  $s_{\text{nematodes}} \sim 25 \text{ mm}^{-2}$ , the highest mean density which is present for the contact angle at which we observe surface deformation, the force per nematode is then given by

$$F_{\text{nematode}} \sim \frac{\Delta p}{s_{\text{nematodes}}} \quad (3)$$

$$\sim 11 \text{ } \mu\text{N}. \quad (4)$$

The two force estimates are similar and consistent with forces measurements of 5 to 30  $\mu\text{N}$  exerted by individual *C. elegans* nematodes that were made using an array of pillars that can bend when pushed by the nematodes [7].

## VI. C. ELEGANS

We sourced the strain *N2* of *C. elegans* grown on agar plates. We followed the same procedures as described above for *T. acetii* to try to obtain a collectively oscillating state. We observed that *C. elegans* exhibit bordertaxis, as already reported in [8], and that individual nematodes oscillate with their heads oriented to the border in a manner similar to *T. acetii*. However, we never saw a synchronization of motion between the nematodes, whatever the nematode concentration and droplet shape and size we tried. An example is shown in supplemental movie SM9 and Figure 3. There are two possible explanations. First, *C. elegans* generally live in soil, and so there may be no evolutionary advantage in collectively driven fluid flows. Secondly, the wider and shorter *C. elegans* has less than a full-wavelength oscillation along the body, and this differs from *T. acetii* which is longer and more slender. It is known [9] that *C. elegans* grown in a liquid medium, as opposed to those grown on agar, are longer and thinner, opening up possibilities for synchronization. However, given the widespread use of *C. elegans* in medical research, it is likely that if a metachronal wave state existed for them, it would have already been noticed and reported.

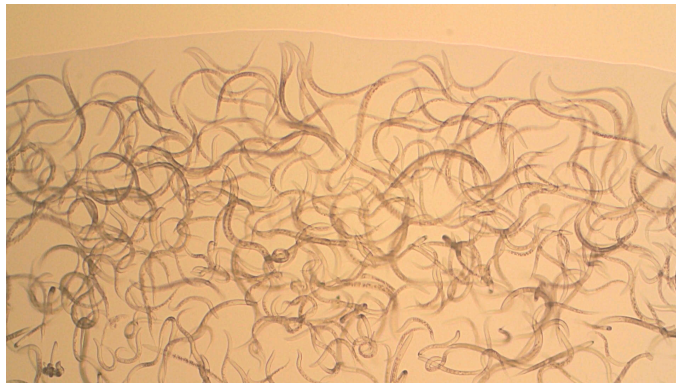


Figure 3. *C. elegans* does exhibit bordertaxis and individual nematodes oscillate at the border. However, no wave is observed.

## VII. SUPPLEMENTAL MOVIES DESCRIPTION

The movies are available at [10]. All movies are in real time, except movie 6.

**Movies:** 1-3: 250  $\mu\text{l}$  droplet at different moments of evaporation. Initial density of nematodes  $d = 30.7 \pm 3.3\text{n}/\mu\text{l}$ .

1. Droplet at time  $t=1$  min. The motion of the nematodes is totally random. Corresponds to figure 1.a) in the main text.

2. Droplet at time  $t=20$  min. Percolation of the metachronal wave. Corresponds to figure 1.b) in the main text.
3. Droplet at time  $t=60$  min. A fully developed metachronal wave move along all the border. Corresponds to figure 1.c) in the main text.

**Movie: 4:** Metachronal wave observed under a microscope with 4x magnification. Corresponds to figure 1.d) in the main text.

**Movie: 5:** A shallow droplet with a formed metachronal wave is observed from the side. The deformation of the surface of the droplet can be seen.

**Movie: 6:** Rotation of fluorescent particles in the central part of the droplet from the flow formed by the nematodes participating in the metachronal wave. The video is accelerated ten times.

**Movie: 7:** Two "defects" in the metachronal wave can be observed which lead to the formation of two counter-rotating metachronal waves. A 750  $\mu\text{l}$  droplet at initial density of nematodes  $d = 15$  n/ $\mu\text{l}$ .

**Movie: 8:** Two counter-rotating waves in consecutive diameters. A 250  $\mu\text{l}$  droplet at initial density of nematodes  $d = 31$  n/ $\mu\text{l}$ .

**Movie: 9:** *C. elegans* observed under a microscope at the border of a droplet. Individual nematodes oscillate at the border, but no synchronization was ever detected.

- 
- [1] M. Kisiel, J. Castillo, L. Zuckerman, B. Zuckerman, and S. Himmelhoch, *Mechanisms of Ageing and Development* **4**, 81 (1975).
  - [2] A. Burr, *Photochemistry and Photobiology* **41**, 577 (1985), doi: 10.1111/j.1751-1097.1985.tb03529.x.
  - [3] A. Stalder, G. Kulik, D. Sage, L. Barbieri, and P. Hoffmann, *Colloids and surfaces A: physicochemical and engineering aspects* **286**, 92 (2006).
  - [4] D. Li, P. Cheng, and A. Neumann, *Advances in Colloid and Interface Science* **39**, 347 (1992).
  - [5] A. Stalder, T. Melchior, M. MÄEler, D. Sage, T. Blu, and M. Unser, *Colloids and Surfaces A: Physicochemical and Engineering Aspects* **364**, 72 (2010).
  - [6] B. Favier, N. Chamakos, and A. Papathanasiou, *Measurement Science and Technology* **28**, 125302 (2017).
  - [7] A. Ghanbari, V. Nock, W. Wang, R. Blaikie, J. Chase, X. Chen, and C. Hann, in *2008 15th International Conference on Mechatronics and Machine Vision in Practice*, edited by anonymous (2008) pp. 634–639.
  - [8] J. Yuan, D. Raizen, and H. Bau, *Journal of The Royal Society Interface* **12**, 20150227 (2015).
  - [9] T. Stiernagle, Maintenance of *c. elegans* (WormBook, 2006) maintenance of *C. elegans*.
  - [10] A. Peshkov, S. McGaffigan, and A. Quillen, <https://doi.org/10.6084/m9.figshare.c.5476659> (2021).